

# Neuropeptides Bombesin and Calcitonin Inhibit Apoptosis-Related Elemental Changes in Prostate Carcinoma Cell Lines

Mercedes Salido, M.D.<sup>1,2</sup>

Jose Vilches, M.D.<sup>2</sup>

Antonio López, M.D.<sup>2</sup>

Godfried M. Roomans, Ph.D.<sup>1</sup>

<sup>1</sup> Department of Medical Cell Biology, University of Uppsala, Uppsala, Sweden.

<sup>2</sup> Department of Cellular Biology, School of Medicine, University of Cádiz, Cádiz, Spain.

**BACKGROUND.** Etoposide-induced apoptosis in prostate carcinoma cells is associated with changes in the elemental content of the cells. The authors previously reported that calcitonin and bombesin inhibited etoposide-induced apoptosis in these cells. In the current study, the authors investigated whether these neuropeptides block the etoposide-induced changes in elemental content.

**METHODS.** Cells from the PC-3 and Du 145 prostate carcinoma cell lines were grown either on solid substrates or on thin plastic films on titanium electron microscopy grids, and they were exposed to etoposide for 48 hours in the absence or presence of calcitonin and bombesin. After the exposure, the cells were frozen and freeze dried, and their elemental content was analyzed by energy-dispersive X-ray microanalysis in both in the scanning electron microscope and the scanning transmission electron microscope.

**RESULTS.** Etoposide treatment consistently induced an increase in the cellular Na concentration and a decrease in the cellular K concentration, resulting in a marked increase of the Na/K ratio and also an increase in the phosphorus:sulphur (P/S) ratio. Both bombesin and calcitonin inhibited the etoposide-induced changes in the cellular Na/K ratio, and calcitonin, but not bombesin, inhibited the changes in the P/S ratio. No significant elemental changes were found with bombesin or calcitonin alone.

**CONCLUSIONS.** The neuropeptides bombesin and calcitonin, which inhibited etoposide-induced apoptosis, also inhibited the etoposide-induced elemental changes in prostate carcinoma cells. This important fact strengthens the link between apoptosis and changes in the intracellular elemental content. This correlation provides an objective basis for the study of neuropeptide target points and may be helpful for alternative therapeutic protocols using neuropeptide inhibitors in the treatment of patients with advanced prostatic carcinoma. *Cancer* 2002;94:368–77. © 2002 American Cancer Society.

**KEYWORDS:** apoptosis, prostate carcinoma, electron probe X-ray microanalysis, bombesin, calcitonin.

Supported in part by grant FIS 01/0727 from the Instituto de Salud Carlos III (Spain).

The authors thank Marianne Ljungkvist and Leif Ljung for excellent technical assistance.

Address for reprints: Mercedes Salido, M.D., Department of Cellular Biology, School of Medicine, University of Cádiz, 1103, Cádiz, Spain; Fax: 34-95601583; E-mail: mercedes.salido@uca.es.

Received May 21, 2001; revision received August 30, 2001; accepted September 19, 2001.

Neuroendocrine differentiation in prostatic malignancy has been associated with a poor prognosis, tumor progression, and androgen independence of the tumor.<sup>1–4</sup> It has been shown that the neuropeptides bombesin and calcitonin can stimulate the growth of prostate carcinoma cell lines.<sup>5–7</sup> In accordance with this, bombesin antagonists inhibit the growth of prostate tumor xenografts in nude mice<sup>8–11</sup> as well as in a rat model of prostate carcinoma.<sup>12</sup> Therefore, it has been suggested that bombesin antagonists may be important in the treatment of patients with advanced prostate carcinoma, especially after they experience disease recurrence.<sup>11,13,14</sup> The mechanism by which bombesin stimulates the growth of prostate carcinoma cells

remains a matter of debate and probably is complex. Bombesin appears to affect various signaling pathways, involving  $\text{Ca}^{2+}$  ions,<sup>15–18</sup> cyclic AMP,<sup>19</sup> and tyrosine kinases, such as Src.<sup>20</sup> It also has been proposed that bombesin may activate extracellular proteolytic activity and, thus, may contribute to metastatic spread.<sup>21</sup> Recently, we showed that bombesin and calcitonin inhibited etoposide-induced apoptosis in prostate carcinoma cell lines,<sup>22</sup> and these neuropeptides, thus, could disrupt the balance between cell death and cell growth in the tumor.

An increase in a neoplastic cell population is the result of imbalance between the two processes controlling tissue homeostasis: cell proliferation and cell death. Apoptosis is associated with specific changes in cell morphology and cellular macromolecules and also is accompanied by changes in ion distribution and membrane potential. In particular, apoptosis is associated with a loss of  $\text{K}^+$  ions from the cell.<sup>23–25</sup> The loss of  $\text{K}^+$  accounts for the changes in cell volume that are associated universally with apoptosis and actually may activate enzymes in the apoptotic cascade<sup>26</sup> and promote DNA degradation.<sup>27</sup> In accordance with these possibilities, increased intracellular  $\text{K}^+$  inhibits apoptosis.<sup>28,29</sup> In addition, other elements may play a role in apoptosis: The level of  $\text{Ca}^{2+}$  is increased (for review, see Mason<sup>30</sup>), and  $\text{Cl}^-$  channels may be activated.<sup>31,32</sup>

We demonstrated previously<sup>22</sup> that combined treatment with etoposide and the neuropeptides bombesin and calcitonin inhibits etoposide-induced apoptosis in these cells, and, in the current study, it was investigated whether these neuropeptides also inhibit the etoposide-induced ionic changes in intracellular ion concentrations in androgen independent cell lines.<sup>33</sup> Understanding how neuropeptides can regulate the ionic fluxes in prostatic androgen-unresponsive tumor cells will be of importance and may prove to be an exciting new target for this disease. Our research interest is focused mainly on those parameters that indicate cell viability ( $\text{Na}/\text{K}$  ratio) and those that reflect alterations in the nuclear-to-cytoplasmic ratio as a result of changes in cell volume and nuclear changes that are described as morphologic hallmarks of apoptosis (phosphorus:sulphur [P/S] ratio and  $\text{Cl}$ ,  $\text{Na}$ , and  $\text{K}$  concentrations). X-ray microanalysis is a useful technique for the study of these changes, in particular, because several elements are analyzed at the same time. This allows the determination of a pattern of elemental changes and of correlations between changes in different elements.

## MATERIALS AND METHODS

### Cell Lines

Two prostatic carcinoma cell lines were used: PC-3, a p53 deficient prostate cell line derived from a bone

metastasis (Nuclear Iberia, Madrid, Spain), and Du 145 (American Type Culture Collection, Rockville, MD), which was derived from a brain metastasis from a prostatic carcinoma.

### Culture Protocols

Cells were grown in Dulbecco modified essential medium (ICN Biomedicals, Aurora, OH) supplemented with 10% fetal bovine serum (FBS; Boehringer, Heidelberg, Germany), 4% penicillin-streptomycin (Biochrom, Berlin, Germany), and 0.4% gentamycin (Gibco, Paisley, Scotland) under standard conditions in a water-saturated atmosphere of 5%  $\text{CO}_2$  until the experiment was started. All experiments were started with unsynchronized, exponentially growing cells, and the culture medium was changed to 5% FBS-supplemented medium.

### Methods

#### *Etoposide-induced apoptosis and its inhibition*

We used the etoposide-induction protocols previously validated in our research group for androgen independent prostate carcinoma cells.<sup>34,35</sup> Briefly, 200,000–500,000 cells per well were seeded in microplates under the conditions described above and, 48 hours later, exposed to etoposide (Sigma, Steinheim, Germany), which was added from a 2-mM stock solution in dimethyl sulfoxide, at doses of 80  $\mu\text{M}$  (Du 145) and 150  $\mu\text{M}$  (PC-3) for 48 hours. To evaluate the inhibition of etoposide-induced apoptosis, cells were exposed to combined treatments with etoposide (as described above) and bombesin 1 nM (Sigma) or calcitonin 500 pg/mL (Sigma).

A control group cultured in the standard medium during the experiment was established in every experiment. Positive controls were treated with bombesin 1 nM or calcitonin 500 pg/mL under the conditions described above.

#### *Apoptosis quantification*

*Direct examination by phase-contrast microscopy.* With a Nikon Diaphot phase-contrast microscope (Nikon, Tokyo, Japan) adapted to a photographic system, we could observe morphologic changes, such as cell surface alterations, blebbing, detachment, and rounding up of treated cells.

*Growth kinetics and cell viability.* Growth kinetics and cell viability were determined by XTT viability assay (Roche, Palo Alto, CA) and trypan blue exclusion with trypan blue in culture media (0.5%). After incubation of cells with trypan blue, nonstained cells were regarded as viable cells, and blue cells were considered nonviable when observed in a hemacytometer. The

percentages of viable cells was defined as the number of nonstained cells  $\div$  total cell number  $\times$  100.

*XTT assay.* Briefly, cells were grown on a microtiter plate with 96 wells and a flat bottom at a final volume of 100  $\mu$ L culture medium per well and in a humidified atmosphere (37 °C, 5% CO<sub>2</sub>) during the assay. After 24 hours and 48 hours, 50  $\mu$ L of the XTT labeling mixture were added to each well. Cells were incubated for 4 hours in a humidified atmosphere, and absorbance of cells was measured using an enzyme-linked immunosorbent assay reader at a wavelength of 450–500 nm.

*Determination of apoptotic process.* For microscopic quantification of apoptotic cells, cytospin preparations obtained from in vitro cell cultures were used as described previously.<sup>22</sup> Briefly, the sample was taken by collecting the supernatant containing the floating apoptotic cells, followed by trypsinization of the rest of the monolayer containing healthy cells. Both fractions were added together to reconstitute the total population and then centrifuged at 1000 rpm for 5 minutes to get the pellet. Cells were then washed twice in phosphate-buffered saline (PBS) and cytospun by means of cytobuckets at 1500 rpm for 5 minutes. Air-dried samples were stained for light, hematoxylin and eosin, and fluorescence microscopy with 4',6'-diamidinonophenylindole.2HCl (DAPI; Boehringer Ingelheim, Heidelberg, Germany).

*Apoptosis staining: (fluorescent DAPI).* Air-dried slides were fixed in metanol at – 20 °C for 20 minutes, air dried, stained with DAPI at room temperature in the dark for 20 minutes, mounted with antifading media (O-phenylenediamine; Sigma, Steinheim, Germany) in glycerol (Merck, Darmstadt, Germany), and preserved in the dark at – 20 °C until examination by fluorescence microscopy at a fluorescence range between 300 nm and 400 nm. The percentage of apoptotic cells was defined as the number of apoptotic cells  $\div$  total cell number  $\times$  100. At least 200 cells were counted for each experiment.

*Apoptosis staining (terminal deoxyuridine triphosphate-biodin nick-end labeling).* Cells were treated as recommended in the kit protocol (Boehringer Mannheim; catalog no. 1684817). Briefly, formalin fixed cells were permeabilized after dehydration and rehydration of the specimens by treatment with 0.5% pepsin, washed in distilled water and Tris-buffered saline (TBS), and endogenous peroxidase was blocked with the blocking solution administered for 30 minutes at room temperature. For the labeling reaction, 50  $\mu$ L of

labeling solution were added to each specimen, except negative controls, for 30 minutes at 37 °C. Then, 50  $\mu$ L of converter POD (antifluorescein antibody conjugated with the reporter enzyme peroxidase [POD]) were then added for 30 minutes at 37 °C, and cells were washed in TBS before the addition of 50  $\mu$ L diaminobenzidine solution for 15 minutes at room temperature. After the washing, cells were counterstained with hematoxylin.

*Flow cytometry.* Cells (10<sup>5</sup>) were centrifuged at 1000 rpm for 5 minutes and washed three times in PBS. The pellet was resuspended in 425  $\mu$ L PBS and 25  $\mu$ L propidium iodide, and 50  $\mu$ L NP40 in 1% PBS were added prior to cytometric analysis (Epics XL; Coulter Cytometry, Hialeah, FL).

*DNA fragmentation.* DNA fragmentation was monitored by a gel electrophoresis method. Briefly, samples of 10<sup>6</sup> cells were washed in PBS and resuspended in 50  $\mu$ L Tris borate ethylenediamine tetracetic acid (EDTA), pH 8.0 (Merck), and 2.4  $\mu$ L Nonidet P40 (Sigma). Then 2  $\mu$ L RNase (1/100; 1 mg/mL; Sigma) were added to each sample prior to incubation at 37 °C for 2 hours. Ten microliters of proteinase k (Boehringer) were added and incubation at 37 °C continuously overnight. Samples were heated to 65 °C, and 20  $\mu$ L agarose were mixed with each sample before loading them into the dry wells of a 2% agarose gel in Tris acetate EDTA  $\times$  1 (Merck). The molecular weight marker was loaded with 4  $\mu$ L marker (Amresco, Solon, OH), 8  $\mu$ L water, and 0.25  $\mu$ L bromophenol blue (Merck) in 10% agarose 1% (Pronadisa, Madrid, Spain). The gels were run at 70 V until the marker dye had migrated 3–4 cm and then at 15 V overnight. DNA was visualized by staining with ethidium bromide (Sigma) and destaining in water.

### X-Ray Microanalysis in the Scanning-Transmission Electron Microscope

For analysis in the scanning transmission electron microscope (STEM), the cells were cultured on titanium grids (Agar Scientific, Stansted, United Kingdom) covered with a Formvar film (Merck). The cells were cultured for 48 hours in the culture medium, as described above, and then exposed to etoposide (150  $\mu$ M), etoposide (150  $\mu$ M) with bombesin (1 nM), etoposide (150  $\mu$ M) with calcitonin (500 pg/mL), bombesin (1 nM), or calcitonin (500 pg/mL) for 48 hours. Control cells were cultured in the standard medium for an additional 48 hours. After the exposure period, the cells on the grids were rinsed briefly in cold distilled water (4 °C), frozen in liquid nitrogen-cooled liquid propane (–180 °C), freeze dried in vacuum

overnight at  $-130\text{ }^{\circ}\text{C}$ , and slowly brought to room temperature under vacuum.<sup>36</sup> Finally, the freeze-dried specimens were coated with a conductive carbon layer. X-ray microanalysis was performed at 100 kV in the STEM mode of a Hitachi (Tokyo, Japan) H7100 electron microscope with an Oxford Instruments ISIS energy-dispersive spectrometer system (Oxford Instruments, Oxford, United Kingdom). Quantitative analysis was carried out based on the peak-to-continuum ratio after correction for extraneous background<sup>37</sup> and by comparing the spectra from the cells with those of a standard, which consisted of known concentrations of mineral salts in a 20% gelatin and 5% glycerol matrix frozen, cryosectioned, and freeze dried to resemble the specimen in its physical and chemical properties.<sup>37</sup> Spectra were acquired for 100 seconds, and only one spectrum was obtained from each cell.

#### X-Ray Microanalysis in the Scanning Electron Microscope

For analysis in the scanning electron microscope (SEM), the cells were grown on Millipore (Bedford, MA) Millicell filters. Culture conditions and exposure to the various substances were that same as those described above for analysis in the STEM. The experiment was terminated by rinsing the filters with the cells in distilled water at  $4\text{ }^{\circ}\text{C}$ . After blotting excess fluid with a filter paper, the cells were frozen immediately in liquid propane cooled by liquid nitrogen and freeze dried overnight at  $-30\text{ }^{\circ}\text{C}$ . The dried filters were coated with a conductive carbon layer to avoid charging in the electron microscope. The cells on the filter were analyzed in a Philips 525 SEM (Philips Electron Optics, Eindhoven, The Netherlands) with a Link AN 10000 energy-dispersive X-ray microanalysis system (Oxford Instruments) at 20 kV. Quantitative analysis was performed by determining the peak-to-background (P/B) ratio of the characteristic intensity (peak; P) to the background intensity (B) in the same energy range as the peak and comparing this P/B ratio with the ratio obtained by analysis of a standard.<sup>37</sup> Each spectrum was acquired for 100 seconds. Only one spectrum was acquired from each cell. No correction for extraneous contributions to the spectrum was applied.

#### Statistical Analysis

Initial statistical comparison of element concentrations was made using an analysis of variance, in which significant differences were established. Homogeneity of means was tested using the Bonferroni test. Correlation coefficients and linear regression equations also

**TABLE 1**  
Percentage of Apoptotic Cells<sup>a</sup>

Treatment	PC-3 cells	Du 145 cells
Control	$7.1 \pm 1.4^b$	$8.8 \pm 2.2^b$
Etoposide	$61.7 \pm 2.59$	$62.0 \pm 1$
Etoposide and bombesin	$33.5 \pm 8.8^c$	$20.4 \pm 2.8^c$
Etoposide and calcitonin	$31.5 \pm 2.8^d$	$45.5 \pm 0.7^b$

<sup>a</sup> The mean  $\pm$  standard deviation values representative of at least ten experiments are given after examination by three independent observers.

<sup>b</sup>  $P = 0.0000$  compared with etoposide-treated cells.

<sup>c</sup>  $P < 0.05$  compared with etoposide-treated cells.

<sup>d</sup>  $P 0.0005$  compared with etoposide-treated cells.

were calculated to assess the strength of the correlations between elements.

## RESULTS

### Characterization of the Apoptotic Process

A flow cytometric study of cell cycle distribution showed an increase of fluorescence in the sub-G1 region and also an accumulation of cells in the G1 area, especially in Du 145 cells, and in G2-M for PC-3 cells, as described previously for etoposide-induced apoptosis. Although cells detached and exhibited classical apoptotic morphology, no subsequent DNA internucleosomal cleavage was observed in Du 145 cells, a cell line that typically exhibits resistance to the production of internucleosomal ladders.

### Inhibition of Etoposide-Induced Apoptosis

The effects of etoposide treatment on the percentage of apoptotic cells with or without added bombesin or calcitonin, according to morphologic examination, is shown in Table 1 for the androgen independent cell lines PC-3 and Du 145. The data show that bombesin and calcitonin inhibit the etoposide-induced increase in the proportion of apoptotic cells.

### Growth Kinetics and Cell Viability

Viability was significantly lower in all etoposide-treated groups compared with the control group. The addition of neuropeptides, as expected, resulted in an increase in cell viability (data not shown).

### X-Ray Microanalysis in the SEM and STEM

Analysis in the STEM showed that, in the Du 145 cell line, etoposide caused a decrease in K and an increase in Na that could be inhibited by bombesin or calcitonin (Fig. 1). Etoposide treatment also caused an increase in the concentration of P and a decrease in S (Fig. 1), resulting in an increase in the ratio of P to S (Fig. 2). This increase was inhibited by calcitonin but

### Du 145

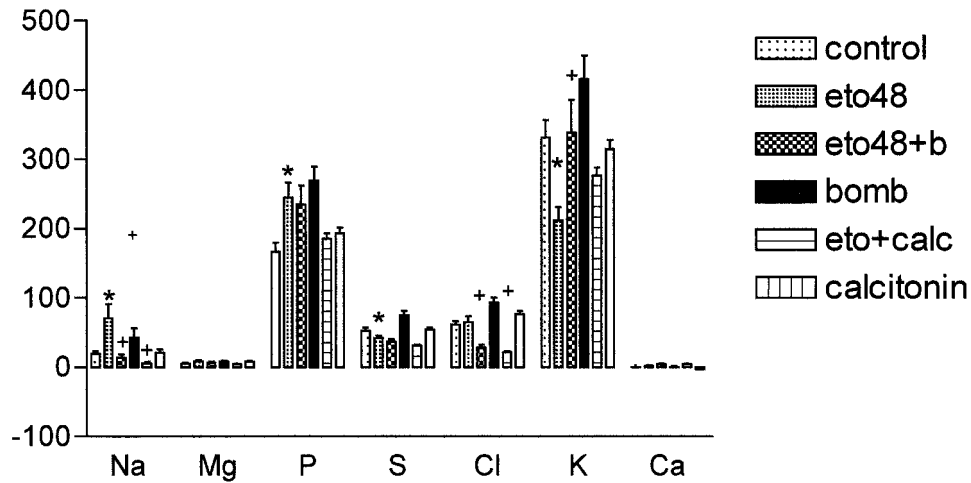


**FIGURE 1.** Elemental concentrations of cells from the Du 145 prostate carcinoma cell line were analyzed in the scanning transmission electron microscope. The mean values (expressed in mmol/kg dry weight) for control cells, cells that were treated for 48 hours with etoposide (eto48), cells that were treated for 48 hours with etoposide in the presence of bombesin (eto48+b), cells that were treated for 48 hours with bombesin alone (bomb), cells that were treated for 48 hours with etoposide in the presence of calcitonin (eto+calc), and cells that were treated for 48 hours with calcitonin alone (calcitonin) are shown. Statistically significant differences between control cells and etoposide-treated cells are denoted by an asterisk ( $P < 0.01$ ), and statistically significant differences between etoposide-treated cells and cells that were treated with etoposide and bombesin or calcitonin are indicated by a cross ( $P < 0.01$ ). Data were based on 25–45 measurements per group from two separate experiments.

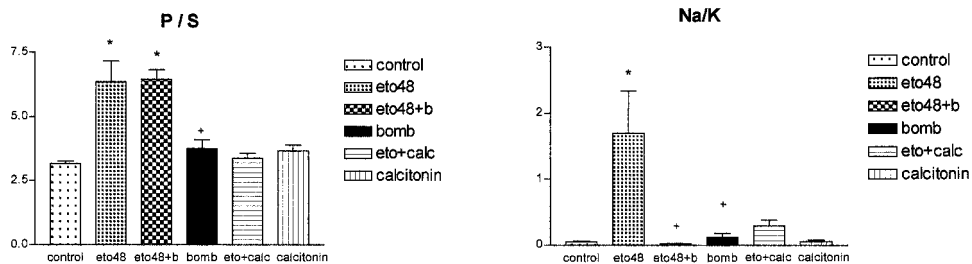


**FIGURE 2.** Elemental ratios in Du 145 cells analyzed in the scanning transmission electron microscope. An increase in the P/S ratio (left) was observed after etoposide treatment that appeared to be blocked by calcitonin. The neuropeptides bombesin and calcitonin blocked an etoposide-induced increase in the Na/K ratio (right). Changes in the P/S ratio can be related to the increased nuclear-to-cytoplasmic ratio that occurs in apoptosis. The increase in intracellular concentrations of Na with respect to K reflects the loss of function of the Na/K pump and, thus, may be regarded as a reliable indicator of the loss of cell viability during apoptosis. Statistically significant differences between control cells and etoposide-treated cells are denoted by an asterisk ( $P < 0.01$ ), and statistically significant differences between etoposide-treated cells and cells that were treated with etoposide and bombesin or with calcitonin are indicated by a cross ( $P < 0.01$ ). Data were based on 25–45 measurements per group from two separate experiments. Control: control cells; eto48: cells that were treated for 48 hours with etoposide; eto48+b: cells that were treated for 48 hours with etoposide in the presence of bombesin; bomb: cells that were treated for 48 hours with bombesin alone; eto+calc: cells that were treated for 48 hours with etoposide in the presence of calcitonin; calcitonin: cells that were treated for 48 hours with calcitonin alone.

not by bombesin (Fig. 2). The Na/K ratio in the Du 145 cells increased markedly after exposure to etoposide, and both bombesin and calcitonin blocked this increase (Fig. 2). However, according to the results from analysis in the SEM (Fig. 3), the cellular P was decreased after etoposide, but the cellular S was decreased even more (Fig. 3). Calculation of the P/S ratio in the SEM measurements confirmed the etoposide-induced increase in the P/S ratio and the fact that this

increase could be inhibited by calcitonin but not by bombesin (Fig. 4). SEM analysis also confirmed the etoposide-induced increase in the Na/K ratio and the inhibition of this increase by both bombesin and calcitonin (Fig. 4). The apparent discrepancy between the increase in P found in the STEM and the decrease in P found in the SEM analysis is explained by the fact that the size of the cells decreases after etoposide treatment (Fig. 5). This means that, in the SEM analysis,

### Du 145

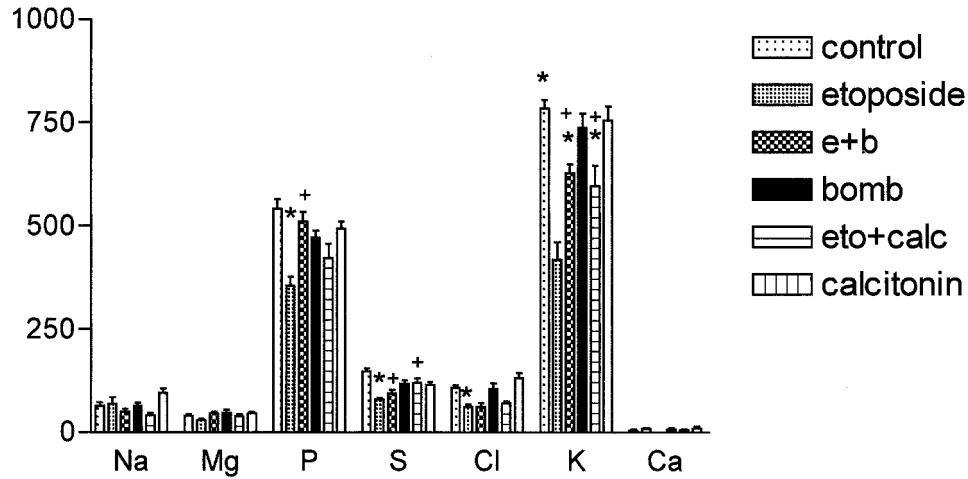


**FIGURE 3.** Elemental concentrations in Du 145 cells analyzed in the scanning electron microscope. Statistically significant differences between control cells and etoposide-treated cells are denoted by an asterisk ( $P < 0.01$ ), and statistically significant differences between etoposide-treated cells and cells that were treated with etoposide and bombesin or calcitonin are indicated by a cross ( $P < 0.01$ ). Data were based on 25–45 measurements per group from two separate experiments. Control: control cells; etoposide: cells that were treated for 48 hours with etoposide; e+b: cells that were treated for 48 hours with etoposide in the presence of bombesin; bomb: cells that were treated for 48 hours with bombesin alone; eto+calc: cells that were treated for 48 hours with etoposide in the presence of calcitonin; calcitonin: cells that were treated for 48 hours with calcitonin alone.

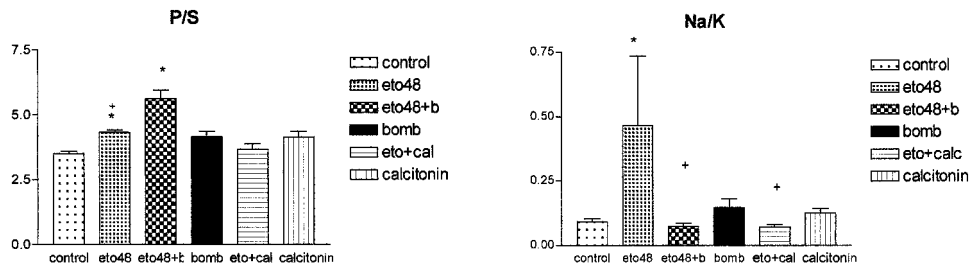


**FIGURE 4.** Elemental ratios in Du 145 cells analyzed in the scanning electron microscope (SEM); left, the P/S ratio; right, the Na/K ratio. Statistically significant differences between control cells and etoposide-treated cells are denoted by an asterisk ( $P < 0.01$ ), and statistically significant differences between etoposide-treated cells and cells that were treated with etoposide and bombesin or with calcitonin are indicated by a cross ( $P < 0.01$ ). Data were based on 25–45 measurements per group from two separate experiments. The discrepancy between scanning transmission electron microscope (STEM) data and SEM data for changes in P concentration likely was due to over-penetration of the electron beam through the shrunken apoptotic cells; therefore, the P/S ratios are shown. The increase in the P/S ratio was blocked by calcitonin but not by bombesin, as observed from the STEM data. Control: control cells; eto48: cells that were treated for 48 hours with etoposide; eto48+b: cells that were treated for 48 hours with etoposide in the presence of bombesin; bomb: cells that were treated for 48 hours with bombesin alone; eto+calc: cells that were treated for 48 hours with etoposide in the presence of calcitonin; calcitonin: cells that were treated for 48 hours with calcitonin alone.

now the substrate also is excited due to over-penetration of the electron beam. The combination of STEM data and SEM data can be interpreted as showing that the amount of P in the cell decreases as a consequence of a decrease in cell size, but that the local concentration of P itself increases relative to other components of the cell.

In the PC-3 cell line, similar results were obtained. Etoposide treatment caused a decrease in P according to the measurements carried out in the SEM but an

increase according to the measurements carried out in the STEM; however, in both cases, the P/S ratio was increased (Fig. 6). This increase was blocked by calcitonin but not by bombesin. Similarly, the Na/K ratio was increased after etoposide treatment, and this increase was blocked by both bombesin and calcitonin.

The cellular K concentration was correlated closely to the P concentration both in control cells (correlation coefficient  $[r^2] = 0.9008$ ) and in etoposide-treated cells ( $r^2 = 0.9580$ ). Also, the Mg concen-

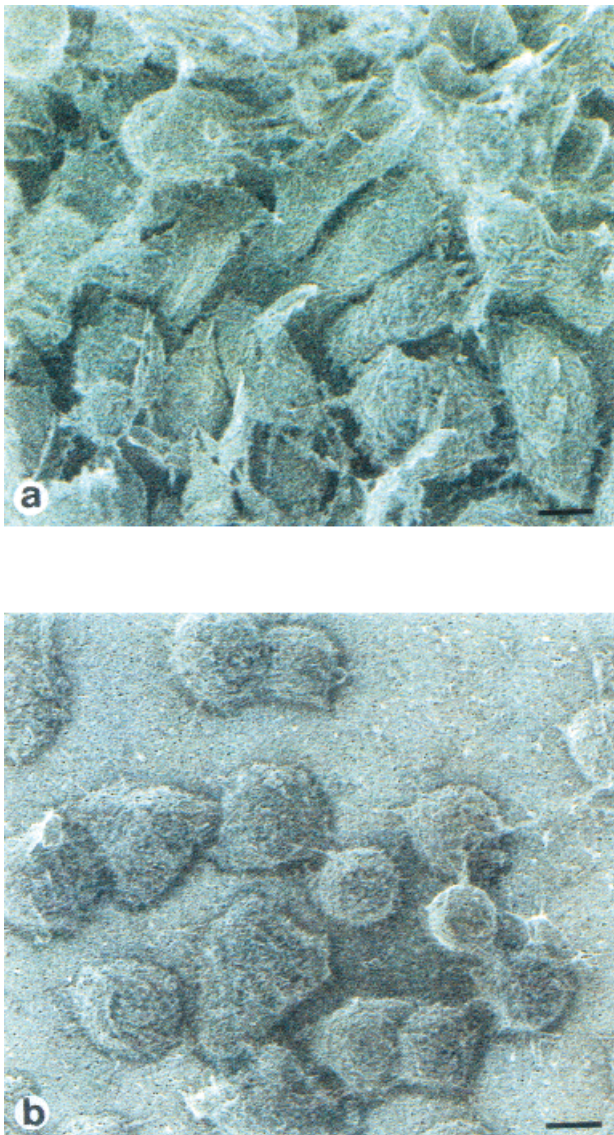


**FIGURE 5.** Scanning electron photomicrographs of Du 145 prostate carcinoma cells (a) control cells and (b) etoposide-treated cells. The photomicrographs show a specimen as it is used for X-ray microanalysis. Briefly, cells were seeded onto polycarbonate tissue culture plate well inserts. Once the experiment was finished, polycarbonate membrane filters were cut from their polystyrene holder and washed with ice-cold, distilled water for 5 seconds. After washing, specimens immediately were plunge-frozen in liquid nitrogen ( $\text{LN}_2$ ), placed in a propane precooled aluminum specimen holder at  $\text{LN}_2$  temperature, and freeze dried overnight at  $-50^\circ\text{C}$  and at  $10_{-1}$  mbar vacuum pressure. The membrane filters were then fixed with adhesive graphite lamina onto stubs and coated with carbon. Scale bars =  $10\ \mu\text{m}$ .

tration was correlated positively with the P concentration. Both for K and for Mg, the significance of the correlation was  $P < 0.001$ . For none of the other elements investigated was there a consistent, significant, positive correlation between the concentration of that

element and the concentration of P. The nature of the correlation between P and K did not change significantly after etoposide treatment, but the range of P and K concentrations was much larger than in the control cells, and the slope of the line describing the correlation decreased.

## DISCUSSION

Apoptosis is associated with a number of changes in the elemental content of the cell. However, the correlation of these elemental changes with the apoptotic process appears complex and has not been elucidated to date. The data from the current study confirm the findings of Fernández-Segura et al.<sup>39</sup> and Skepper et al.<sup>40</sup> that apoptosis is associated with an increase in cellular Na and a decrease in cellular K concentrations. Several studies have shown that loss of  $\text{K}^+$  is associated with apoptosis.<sup>23,24,26</sup> It has been suggested that this loss of  $\text{K}^+$  may be secondary to a disruption of mitochondrial activity.<sup>23,28,38</sup> Indeed, it can be speculated that the disruption of mitochondrial activity may result in decreased levels of ATP, with the consequence of reduced activity of  $\text{Na}^+/\text{K}^+$ -ATPase, which would explain the simultaneous increase in  $\text{Na}^+$  levels and the decrease in  $\text{K}^+$  levels. However, this notion would be difficult to reconcile with the results of Fernández-Segura et al.<sup>39</sup> showing that the changes in the cellular Na/K ratio were not associated with the loss of cell membrane integrity. It also has been suggested that the reduction in cell size that is one of the hallmarks of apoptosis may be accompanied by an efflux of  $\text{Cl}^-$  and  $\text{K}^+$  ions through volume-regulating ion channels.<sup>31,41</sup> Efflux of chloride ions during apoptosis has been found previously but has been attributed to outwardly rectifying chloride channels or chloride-bicarbonate exchange.<sup>28,32,42,43</sup> Whether the cellular chloride concentration decreases significantly during apoptosis is not entirely clear from our data. Whereas analysis in the SEM (Fig. 3; see also Salido et al.<sup>33</sup>) shows a lower intracellular chloride concentration in apoptotic cells, analysis in the STEM (Fig. 1) does not show a significant change in intracellular chloride during apoptosis.

When cells are grown on a solid substrate and analyzed in the SEM, there is a theoretic possibility that the electron beam penetrates the cell entirely and excites the substrate. The likelihood for this increases when the cell shrinks, which is the case during apoptosis. This implies that a measured decrease in elemental concentration under such conditions can be due in part to a decrease in cell size. This possible artifact has to be taken into account in the interpretation of data obtained by analysis of cells on a solid substrate.<sup>39,41</sup> Analysis of cells grown on thin plastic

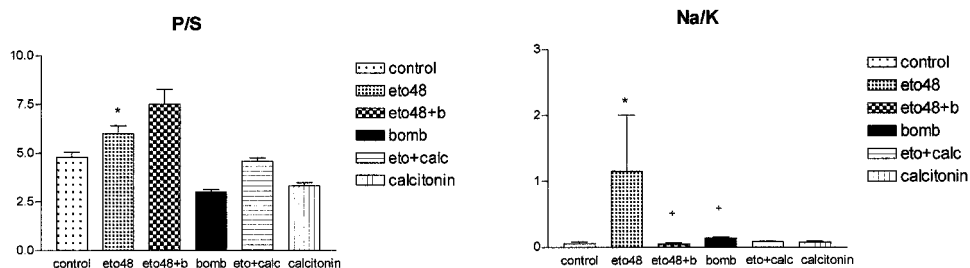


**FIGURE 6.** Elemental ratios in PC-3 cells analyzed in the scanning electron microscope: left, the P/S ratio; right, the Na/K ratio. Similar results were obtained in scanning transmission electron microscope analysis. Statistically significant differences between control cells and etoposide-treated cells are denoted by an asterisk ( $P < 0.01$ ), and statistically significant differences between etoposide-treated cells and cells that were treated with etoposide and bombesin or with calcitonin are indicated by a cross ( $P < 0.01$ ). Data were based on 30–60 measurements per group from three separate experiments. Control: control cells; eto48: cells that were treated for 48 hours with etoposide; eto48+b: cells that were treated for 48 hours with etoposide in the presence of bombesin; bomb: cells that were treated for 48 hours with bombesin alone; eto+calc: cells that were treated for 48 hours with etoposide in the presence of calcitonin; calcitonin: cells that were treated for 48 hours with calcitonin alone.

films on grids in the STEM avoids these problems, although the method, as such, is more difficult technically.<sup>44,45</sup> A comparison of the two methods<sup>46</sup> showed that systematic errors in the absolute concentrations could be introduced easily in both methods but that elemental ratios would be relatively free of such artifacts. In the current report, therefore, data also were expressed as elemental ratios, and the direction of the changes is the same in both types of measurement (cf. Figs. 2 and 4).

The data indicate that apoptosis is associated with a relative increase in P, in particular, with an increase in the P/S ratio. This has not been noted previously: The study by Fernández-Segura et al.<sup>39</sup> indicated a small increase in P but provided no data for S. Cellular P is almost exclusively in the form of phosphates, most of which are bound in macromolecules (DNA, RNA, and large organic phosphates), whereas cellular S is indicative of the protein content of the cell. The most likely explanation of the increase in the P/S ratio is that it is related to the well-known relative increase of the nuclear-to-cytoplasmic ratio that occurs during apoptosis. Whether additional factors, such as changes in the type or distribution of nucleic acids and/or changes in the types of amino acids incorporated in proteins, are involved will require further study. Our data, however, do provide an indication that the situation may be quite complex. There was a correlation between the cellular concentrations of P and K, both in control cells and in etoposide-treated cells. In many X-ray microanalytic studies of rapidly growing cells or tumor cells, parallel changes in P and K (and Mg) have been noted.<sup>47–49</sup> This often has been attributed to the fact that  $K^+$  and  $Mg^{2+}$  are the preferred counterions for phosphate groups. However, the  $r$  value for the linear correlation between elements

also indicates that etoposide treatment induced a reduction in the slope of the line that can be constructed for the relationship between P and K, which may point to a change in the distribution of the negatively charged phosphate groups in nucleic acids during apoptosis.

The mechanism of the  $K^+$  loss associated with apoptosis, as discussed above, is still being debated. In addition, there are indications that  $K^+$  loss is not just a consequence of apoptosis but that, in itself, it may promote apoptosis, because caspases and nucleases are inhibited by high intracellular  $K^+$ , and inhibition of  $K^+$  efflux results in the inhibition of apoptosis.<sup>26–29,50–52</sup> Both bombesin and calcitonin, which inhibit etoposide-induced apoptosis in prostate carcinoma cells, also inhibit fully the etoposide-induced changes in the Na/K ratio. This in itself does not provide information on whether the etoposide-induced change in the Na/K ratio is the cause or the effect (or both) of apoptosis, but it strengthens the link between the elemental changes in cellular ion content and the apoptotic process. Calcitonin, but not bombesin, also reverses the etoposide-induced changes in the P/S ratio. Because the change in the P/S ratio probably is multifactorial, an explanation for this difference cannot be provided currently but requires further study.

It can be concluded that apoptosis is associated strongly with changes in the intracellular concentration of several elements. It also has been shown that X-ray microanalysis is a useful technique to study these changes, in particular, because several elements are analyzed at the same time. This allows the determination of a pattern of elemental changes and of correlations between changes in different elements.

The current study confirms and extends our pre-

vious work in this area and confirms the finding that the neuropeptides that inhibit etoposide-induced apoptosis also inhibit the etoposide-induced elemental changes in the cells. Neuropeptide-induced resistance to etoposide-induced apoptosis represents a new mechanism-based approach that may help to identify novel drugs and/or develop new therapeutic regimens for the treatment of patients with prostate carcinoma, using these neuropeptides secreted by prostatic cells implied in prostatic carcinoma as a target in tumor therapy. Our findings suggest the merit of further studies to investigate the point at which the etoposide-induced events described above may interact with bombesin or calcitonin signal-transduction pathways and to evaluate the possible usefulness of antagonists of bombesin in the management of patients with prostatic carcinoma. The PC-3 and Du 145 human prostate carcinoma cell lines possess specific high-affinity receptors for bombesin/gastrin-releasing peptide (GRP) and have been used as suitable models for the evaluation of the antineoplastic activity of bombesin/GRP antagonists in the treatment of patients with androgen independent prostate carcinoma.<sup>11,53-57</sup>

## REFERENCES

- Ather MH, Abbas F. Prognostic significance of neuroendocrine differentiation in prostate cancer. *Eur Urol* 2000;38:535-42.
- di Sant'Agnese PA. Divergent neuroendocrine differentiation in prostatic carcinoma. *Semin Diagn Pathol* 2000;17:149-61.
- Abrahamsson PA. Neuroendocrine differentiation in prostatic carcinoma. *Prostate* 1999;39:135-48.
- di Sant'Agnese PA. Neuroendocrine differentiation in prostatic carcinoma: an update. *Prostate* 1998;8(Suppl):74-9.
- Ritchie CK, Thomas KG, Andrews LR, Tindall DJ, Fitzpatrick LA. Effects of the calciotropic peptides calcitonin and parathyroid hormone on prostate cancer growth and chemotaxis. *Prostate* 1997;30:183-7.
- Shah GV, Rayford W, Noble MJ, Austenfeld M, Weigel J, Vamos S, et al. Calcitonin stimulates growth of human prostate cancer cells through receptor-mediated increase in cyclic adenosine 3',5'-monophosphates and cytoplasmic Ca<sup>2+</sup> transients. *Endocrinology* 1994;134:596-602.
- Bologna M, Festuccia C, Muzi P, Biordi L, Ciomei M. Bombesin stimulates growth of human prostatic cancer cells in vitro. *Cancer* 1989;63:1714-20.
- Pinski J, Schally AV, Halmos G, Szepeshazi K. Effect of somatostatin analog RC-160 and bombesin/gastrin releasing peptide antagonist RC-3095 on growth of PC-3 human prostate-cancer xenografts in nude mice. *Int J Cancer* 1993;55:963-7.
- Pinski J, Halmos G, Schally AV. Somatostatin analog RC-160 and bombesin/gastrin-releasing peptide antagonist RC-3095 inhibit the growth of androgen-independent Du-145 human prostate cancer line in nude mice. *Cancer Lett* 1993;71:189-96.
- Plonowski A, Schally AV, Varga JL, Rekasi Z, Hebert F, Halmos G, et al. Potentiation of the inhibitory effect of growth hormone-releasing hormone antagonists on PC-3 human prostate cancer by bombesin antagonists indicative of interference with both IGF and EGF pathways. *Prostate* 2000;44:172-80.
- Jungwirth A, Pinski J, Galvan G, Halmos G, Szepeshazi K, Cai RZ, et al. Inhibition of growth of androgen-independent Du-145 prostate cancer in vivo by luteinising hormone-releasing hormone antagonist Cetrorelix and bombesin antagonists RC-3940-II and RC-3950-II. *Eur J Cancer* 1997;33:1141-8.
- Plonowski A, Nagy A, Schally AV, Sun B, Groot K, Halmos G. In vivo inhibition of PC-3 human androgen-independent prostate cancer by a targeted cytotoxic bombesin analogue, AN-215. *Int J Cancer* 2000;15:652-7.
- Pinski J, Reile H, Halmos G, Groot K, Schally AV. Inhibitory effects of somatostatin analogue RC-160 and bombesin/gastrin-releasing peptide antagonist RC-3095 on the growth of the androgen-independent Dunning R-3327-AT-1 rat prostate cancer. *Cancer Res* 1994;54:169-74.
- Schally AV, Comaru-Schally AM, Plonowski A, Nagy A, Halmos G, Rekasi Z. Peptide analogs in the therapy of prostate cancer. *Prostate* 2000;45:158-66.
- Han K, Viallet J, Chevalier S, Zheng W, Bazinet M, Aprikian AG. Characterization of intracellular calcium mobilization by bombesin-related neuropeptides in PC-3 human prostate cancer cells. *Prostate* 1997;31:53-60.
- Wasilenko WJ, Cooper J, Palad AJ, Somers KD, Blackmore PF, Rhim JS, et al. Calcium signaling in prostate cancer cells: evidence for multiple receptors and enhanced sensitivity to bombesin/GRP. *Prostate* 1997;30:167-73.
- Wertz IE, Dixit VM. Characterization of calcium release-activated apoptosis of LNCaP prostate cancer cells. *J Biol Chem* 2000;275:11470-7.
- Aprikian AG, Han K, Chevalier S, Bazinet M, Viallet J. Bombesin specifically induces intracellular calcium mobilization via gastrin-releasing peptide receptors in human prostate cancer cells. *J Mol Endocrinol* 1996;16:297-306.
- Jongsma J, Oomen MH, Noordzij MA, Romijn JC, van der Kwast TH, Schröder FH. Androgen-independent growth is induced by neuropeptides in human prostate cancer cell lines. *Prostate* 2000;42:34-44.
- Allard P, Beaulieu P, Aprikian A, Chevalier S. Bombesin modulates the association of Src with a nuclear 110-kd protein expressed in dividing prostate cells. *J Androl* 2000;21:367-75.
- Festuccia C, Guerra F, D'Ascenzo S, Giunciuglio D, Albini A, Bologna M. In vitro regulation of pericellular proteolysis in prostatic tumor cells treated with bombesin. *Int J Cancer* 1998;75:418-31.
- Salido M, Vilches J, Lopez A. Neuropeptides bombesin and calcitonin induce resistance to etoposide induced apoptosis in prostate cancer cell lines. *Histol Histopathol* 2000;15:729-38.
- Dallaporta B, Hirsch T, Susin SA, Zamzami N, Larochette N, Brenner C, et al. Potassium leakage during the apoptotic degradation phase. *J Immunol* 1998;160:5605-15.
- Dallaporta B, Marchetti P, de Pablo MA, Maise C, Duc HT, Metivier D, et al. Plasma membrane potential in thymocyte apoptosis. *J Immunol* 1999;162:6534-42.
- Bortner CD, Hughes FM Jr., Cidlowski JA. A primary role for K<sup>+</sup> and Na<sup>+</sup> efflux in the activation of apoptosis. *J Biol Chem* 1997;272:32436-42.

26. Hughes FM Jr., Cidlowski JA. Potassium is a critical regulator of apoptotic enzymes in vitro and in vivo. *Adv Enzyme Regul* 1999;39:157-71.
27. Montague JW, Bortner CD, Hughes FM Jr., Cidlowski JA. A necessary role for reduced intracellular potassium during the DNA degradation phase of apoptosis. *Steroids* 1999;64:563-9.
28. Yu SP, Choi DW. Ions, cell volume, and apoptosis. *Proc Natl Acad Sci USA* 2000;97:9360-2.
29. Hughes FM Jr., Bortner CD, Purdy GD, Cidlowski JA. Intracellular  $K^+$  suppresses the activation of apoptosis in lymphocytes. *J Biol Chem* 1997;272:30567-76.
30. Mason RP. Calcium channel blockers, apoptosis and cancer: is there a biologic relationship? *J Am Coll Cardiol* 1999;34:1857-66.
31. Maeno E, Ishizaki Y, Kanaseki T, Hazama A, Okada Y. Normotonic cell shrinkage because of disordered volume regulation is an early prerequisite to apoptosis. *Proc Natl Acad Sci USA* 2000;97:9487-92.
32. Szabo I, Lepple-Wienhues A, Kaba KN, Zoratti M, Gulbins E, Lang F. Tyrosine kinase-dependent activation of a chloride channel in CD95-induced apoptosis in T lymphocytes. *Proc Natl Acad Sci USA* 1998;95:6169-74.
33. Salido M, Vilches J, López A, Roomans GM. X-ray microanalysis of etoposide induced apoptosis in the Pc-3 prostatic cancer cell line. *Cell Biol Int* 2001;25:499-508.
34. Salido M, López A, Aparicio J, Larrán J, Vilches J. Characterization of apoptosis in prostatic androgen independent cell lines. *Int J Dev Biol* 1996;1(Suppl):191-2.
35. Salido M, Larrán J, Vilches J, López A, Aparicio J. Etoposide sensitivity of human prostatic cancer cell lines PC-3, Du 145, LNCaP. *Histol Histopathol* 1999;14:125-34.
36. Zhang W, Roomans GM. Volume induced chloride transport in HT29 cells studied by X-ray microanalysis. *Microsc Res Techn* 1998;40:72-8.
37. Roomans GM. Quantitative X-ray microanalysis of biological specimens. *J Electron Microsc Techn* 1988;9:19-44.
38. Kroemer G, Dallaporta B, Resche-Rigon M. The mitochondrial death/life regulator in apoptosis and necrosis. *Annu Rev Physiol* 1998;60:619-42.
39. Fernández-Segura E, Cañizares FJ, Cubero MA, Warley A, Campos A. Changes in elemental content during apoptotic cell death studied by electron probe X-ray microanalysis. *Exp Cell Res* 1999;253:454-62.
40. Skepper JN, Karydis I, Garnett MR, Hegyi L, Hardwick SJ, Warley A, et al. Changes in elemental concentrations are associated with early stages of apoptosis in human monocyte-macrophages exposed to oxidized low-density lipoprotein: an X-ray microanalytical study. *J Pathol* 1999;188:100-6.
41. Warley A, Arrebola, F, Zabiti S, Cañizares F, Cubero MA, Fernández-Segura E, et al. Changes in sodium, chloride and potassium during apoptotic cell death. An X-ray microanalytical study. In: Frank L, Čiampor F, editors. Proceedings of the 12th European Congress on Electron Microscopy. Brno: Czechoslovak Society on Electron Microscopy, 2000:B427-8.
42. Fujita H, Ishizaki Y, Yanagisawa A, Morita I, Murota SI, Ishikawa K. Possible involvement of a chloride-bicarbonate exchanger in apoptosis of endothelial cells and cardiomyocytes. *Cell Biol Int* 1999;23:241-9.
43. Fujita H, Yanagisawa A, Ishikawa K. Suppressive effect of a chloride bicarbonate exchanger inhibitor on staurosporine-induced apoptosis of endothelial cells. *Heart Vessels* 1997;12(Suppl):84-8.
44. Von Euler A, Pålsgård E, Vult von Steyern C, Roomans GM. X-ray microanalysis of epithelial and secretory cells in culture. *Scanning Microsc* 1993;7:191-202.
45. Roomans GM, Hongpaisan J, Jin Z, Mörk AC, Zhang A. In vitro systems and cultured cells as specimens for X-ray microanalysis. *Scanning Microsc* 1996;10(Suppl):359-74.
46. Roomans GM. X-ray microanalysis of cultured cells in the scanning electron microscope and the scanning transmission electron microscope: a comparison. *Scanning Microsc* 1999;13:159-65.
47. Grundin TG, Roomans GM, Forslind B, Lindberg M, Werner Y. X-ray microanalysis of psoriatic skin. *J Invest Dermatol* 1985; 85:378-80.
48. Grängsjö A, Ybo A, Roomans GM, Lindberg M. Irritant-induced keratinocyte proliferation evaluated with two different methods: immunohistochemistry and X-ray microanalysis. *J Submicrosc Cytol Pathol* 2000;32:11-6.
49. Smith NKR, Cameron IL. Ionic regulation of proliferation in normal and cancer cells. In: Ingram P, Shelburne JD, Roggli VL, LeFurgey A, editors. Biomedical applications of microprobe analysis. San Diego: Academic Press, 1999:445-59.
50. Watson RW, Fitzpatrick JM. Target sites for manipulating apoptosis in prostate cancer. *Br J Urol* 2000;85(Suppl):38-44.
51. Johnson VL, Ko SC, Holmstrom TH, Erikssohn JE, Chow SC. Effector caspases are dispensable for the early nuclear morphological changes during chemical-induced apoptosis. *J Cell Sci* 2000;113:2941-53.
52. Coffey RNT, Watson RW, Fitzpatrick JM. Signaling for the caspases: their role in prostate cell apoptosis. *J Urol* 2001;165:5-14.
53. Reile H, Armatis PE, Schally AV. Characterization of high-affinity receptors for bombesin/gastrin releasing peptide on the human prostate cancer cell lines PC-3 and Du 145: internalization of receptor bound 125I-(Tyr4) bombesin by tumor cells. *Prostate* 1994;25:29-38.
54. Jungwirth A, Galvan G, Pinski J, Halmos G, Szepeshazi K, Cai RZ, et al. Luteinizing hormone-releasing hormone antagonist Cetrorelix (SB-75) and bombesin antagonist RC-3940-II inhibit the growth of androgen-independent PC-3 prostate cancer in nude mice. *Prostate* 1997;32:164-72.
55. Milovanovic SR, Radulovic S, Groot K, Schally AV. Inhibition of growth of PC-82 human prostate cancer cell line xenografts in nude mice by bombesin antagonist RC-3095 or combination of agonist [D-Trp6]-luteinizing hormone-releasing hormone and somatostatin analog RC-160. *Prostate* 1992;20:269-80.
56. Imam H, Eriksson B, Lukinius AA, Janson ET, Lindgren PG, Wilander E, et al. Induction of apoptosis in neuroendocrine tumors of the digestive system during treatment with somatostatin analogs. *Acta Oncol* 1997;36:607-14.
57. Zhang RS, Degrot LL. A monoclonal antibody against rat calcitonin inhibits the growth of a rat medullary thyroid carcinoma cell line in vitro. *Endocrinology* 1997;138:1697-703.